Stagnant recrystallization in warm-rolled tungsten in the temperature range from 1150 °C to 1300 °C

Ciucani, Umberto Maria; Pantleon, Wolfgang

Published in:
Fusion Engineering and Design

Link to article, DOI:
10.1016/j.fusengdes.2019.01.088

Publication date:
2019

Document Version
Peer reviewed version

Stagnant recrystallization in warm-rolled tungsten in the temperature range from 1150 °C to 1300 °C

Umberto Maria Ciucani, Wolfgang Pantleon.

Section for Materials and Surface Engineering, Department of Mechanical Engineering, Technical University of Denmark, 2800 Kongens Lyngby, Denmark.

Pure tungsten is the prime candidate for armor material of fusion reactors; its application at the expected operation temperatures for longer times will result in changes in the microstructure, in particular due to recrystallization, undermining the otherwise outstanding properties of tungsten. Investigating the thermal stability of tungsten depending on the manufacturing technology is therefore crucial. The thermal response of a sintered, hot isostatically pressed tungsten plate warm-rolled to 80% thickness reduction is assessed in the temperature range between 1150 °C and 1300 °C. Isothermal annealing treatments were performed at six different temperatures. With increasing annealing time, the macro hardness decreased and different stages corresponding to different stages of the microstructural evolution and the progress of recrystallization could be identified and confirmed by electron backscatter diffraction. For all six annealing temperatures a stagnation period in the evolution of the macro hardness was observed where the degradation of mechanical properties halted for a significant amount of time, before it resumed. Microstructural investigations revealed that the stagnation occurred when tungsten was still only partially recrystallized. For the time to half recrystallization, an activation energy of 548 kJ/mol comparable to the activation energy of bulk self-diffusion is inferred.

Keywords: tungsten; rolling; annealing; recrystallization; thermal stability; hardness testing.

1. Introduction

Tungsten is considered the prime candidate for the armour material of plasma-facing components of future fusion reactors as it combines high thermal conductivity, high yield stress, strength, and creep resistance even at high temperatures [1,2]. In particular, its high melting temperature enables tungsten to withstand the high heat loads, high temperatures and temperature gradients arising at the first wall and the divertor [3]. For a safe operation, non-brittle behaviour of the material between room and operation temperature is desired. This can be achieved by severe plastic deformation, as tungsten in a deformed state behaves rather ductile [1,4]. At the high stationary operation temperatures (up to 1200 °C [3] at the divertor), the microstructure of the material will be altered by recovery and recrystallization, degrading eventually the mechanical properties. During recrystallization the undeformed, polycrystalline state is reinstated. The dislocation-free, almost equiaxed grain structure is characterized by lower strength than the deformed state and a brittle behaviour caused by incompatible plastic deformation at grain boundaries[1,5-6]. By selecting proper manufacturing conditions, the microstructure of tungsten can be tailored and its thermal stability ought to be improved. Several studies on thermal stability and recrystallization of pure tungsten plates and foils rolled to different reductions have been reported [7-15].

The work presented here investigated the thermal stability of tungsten warm-rolled to an intermediate rolling reduction (80%) in comparison with two earlier investigations on lower (67%) [7] and higher (90%) [8] rolling reductions which showed a significant difference in their recrystallization kinetics. The most important finding is the discovery of an incomplete recrystallization even upon annealing at high temperatures for long periods of time. Such a stagnation in the recrystallization process may provide guidance towards materials with an improved thermal stability.

2. Materials and Methods

The thermal stability of warm-rolled 99.95% pure tungsten was investigated on a plate with dimensions 200.8 x 100.3 x 8.3 mm^3 along rolling direction (RD), transversal direction (TD) and normal direction (ND), respectively. The plate (termed W80) has been manufactured by Advanced Technology & Materials Co. Ltd. in Beijing using a powder metallurgical route (sintering and hot isostatic pressing) followed by warm-rolling to a thickness reduction of 80% to be compared with two earlier investigated plates warm-rolled to 67% (W67 [7]) and 90% thickness reduction (W90 [8]). From the plate, small specimens (6 x 5 x 4 mm^3 along RD, TD and ND, respectively) were cut for annealing. They were encapsulated in sealed quartz glass tubes flushed by Argon to prevent oxidation of tungsten and the formation of volatile oxides. Isothermal annealing treatments were performed in a general-purpose tube furnace NaberTherm RHTC 80-230/15 at six different temperatures ranging from 1150 °C to 1300 °C for different time spans as long as 1872 h (i.e. 78 days) to assess the thermal stability and the recrystallization behaviour of W80. Additionally, two samples were annealed at even higher temperatures (1350 °C and 1400 °C) to ensure full recrystallization.

The progress of the microstructural evolution was traced by Vickers hardness testing of the annealed specimens in comparison to the as-received condition. The macro hardness of the as-received plate was tested on both open rolling surfaces with a load of 10 kgf. After cutting the plate into bars with a size of 6 mm along RD, micro hardness mapping of several TD/ND sections was performed using a smaller load of 0.5 kgf, additional to macro hardness testing (HV10). For the annealed specimens, macro hardness tests with a load of 10 kgf were performed solely on TD/ND sections. For each condition, 24 macro indents were analysed (with the exception of 1250 °C and 1300 °C where a lower number, but at least 10 macro indents, were performed for each condition). Discarding the smallest and the largest hardness value measured, the resulting average hardness are reported together with the standard deviation of the average.

For a concise characterization of the microstructure, orientation mapping is employed using electron backscatter diffraction. EBSD investigations were

author's email: umciuc@mek.dtu.dk

performed with Bruker Esprit software on a FEI NOVA NanoSEM 600 using an applied voltage of 20 kV and a step size of 500 nm for the as-received condition and 2 µm for the annealed ones. For each annealed condition, two orientation maps of 792 µm × 660 µm on the RD/ND section adjacent to each other along ND were acquired and combined into a single map slightly smaller than 792 µm x 1320 µm due to the required overlap for stitching. Both, macro hardness testing and orientation mapping were performed as close as possible to the centre of the plate with respect to ND, i.e. in the region furthest away from contact with the rolls.

3. Results

3.1 As-received condition

Macro hardness testing of the as-received plate on both rolling surfaces revealed a substantial heterogeneity in the hardness distribution. This was further substantiated by micro hardness mapping of TD/ND sections after cutting into bars along RD. By mapping several TD/ND sections, reasonably large regions in the plate of homogeneous hardness could be identified. The relatively constant hardness value of these regions of 437±2 HV10 is taken as hardness of the as-received condition; it is quite similar to the hardness of the earlier investigated plates, i.e. 423±4 HV10 for W67 [7] and 434±2 HV10 for W90 [8]. In order to minimize the effect of the heterogeneous hardness in the plate, specimens for the annealing experiments were cut solely from regions where a constant hardness is expected from the micro hardness mapping of neighboring regions.

Orientation maps on RD/ND sections of the regions with homogeneous hardness in the as-received condition (not shown here) revealed the presence of a partially recrystallized structure after warm-rolling. Even before any annealing, almost equiaxed, recrystallized grains accounting for a recrystallized volume fraction X_V of (18±2)% were observed alongside with elongated and fragmented grains representing the deformed structure.

3.2 Hardness evolution during isothermal annealing

The hardness evolution during isothermal annealing between 1150 °C and 1300 °C is summarized in Fig. 1. During annealing, the macro hardness decreases gradually from the value 437±2 HV10 of the as-received condition (the black point in Fig. 1) to the much lower hardness of the recrystallized condition. The hardness value of 357±2 HV10 considered representative for the fully recrystallized condition was obtained as an average of several conditions at different annealing temperatures (illustrated by the bottom grey band of Fig. 1) for which complete recrystallization could be presumed and confirmed by EBSD investigations (see e.g. Fig. 2a). The occasionally observed intermittent increase in hardness is considered to be unphysical and ignored; it is attributed to the use of individual samples for each data point and the heterogeneity of the initial condition in the plate which was not be completely eliminated by selecting samples from proper regions.

The overall evolution (even ignoring any non-monotonous behaviour) does not follow the commonly observed trend with an initial, slight decrease slowing down with annealing time due to recovery, continued by a more severe decrease following a sigmoidal curve characteristic for recrystallization (see for instance [7,8]). Instead the decrease in hardness seems to come to a temporary halt. The most obvious halting period occurs at a macro hardness level of about 390±10 HV10 (marked as the middle one of the grey bands in Fig. 1), a similar halting period may be seen at 417±7 HV10 at least for the three lowest temperatures (top grey band in Fig. 1). After the initial decrease to 417±7 HV10 and halt, the hardness decreases relatively suddenly to the lower halting value of 390±10 HV10. At this hardness value, the hardness

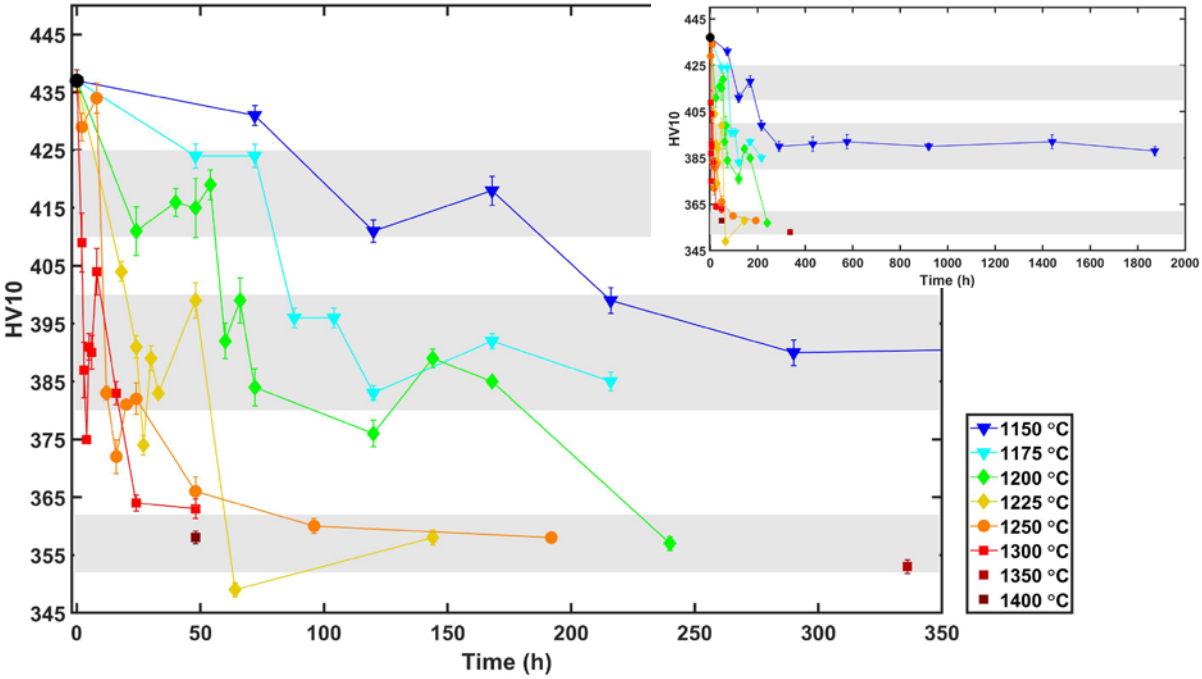

Fig. 1: Hardness evolution during annealing of tungsten warm-rolled to 80% thickness reduction (W80). Symbols and error bars mark average hardness value and their standard deviations. The three grey bands highlight the intermediate halting periods.

evolution stagnates for a considerable amount of time without any further reduction (at least for the four annealing experiments at the lowest temperatures between 1150 °C and 1225 °C; at 1250 °C stagnation occurs at slightly lower hardness). For all except the two lowest annealing temperatures, the hardness finally decreases to the value 357±2 HV10 of the fully recrystallized condition (for 1200 °C after 200 h, for 1250 °C after 50 h and at 1300 °C from 24 h).

3.3 Microstructure evolution during annealing

The peculiarities in the hardness evolution during annealing relate to the underlying microstructure evolution. Fig. 2a shows the microstructure of a sample annealed for 192 h at 1250 °C as obtained by EBSD; the orientation map reveals an abundance of defect-free, almost equiaxed grains. Only in small regions, remains of the deformation structure can be traced; the structure is (almost) fully recrystallized. From the EBSD data, a recrystallized volume fraction X_V of (99±1)% is determined, which is confirmed by the low hardness value 358±1 HV10. Fig. 2b, on the other hand, shows the microstructure after annealing for 1872 h at 1150 °C. Despite the rather long annealing time (the longest in the entire study, about 2.5 months), the sample has not fully recrystallized and the recrystallized volume fraction X_V is only (65±2)%. After the stagnation value of about 390 HV10 is attained after 286 h at this temperature, the hardness almost does not change during the following 1500 h (two months) (see insert in Fig. 1). Several samples annealed for different times at different temperatures with a hardness value corresponding to this stagnation value (390±10 HV) have been investigated and their microstructure analysed by EBSD. The vast majority of them resulted in a recrystallized volume fraction between 60% and 80% as determined from the orientation maps. In a similar manner, samples with a hardness value of 417±7 HV10 corresponding to the first apparent period of stagnation showed a recrystallized volume fraction about 40% proving that also the initial hardness drop is caused by progress in recrystallization from the partially recrystallized, as-received condition.

3.4 Annealing kinetics

The hardness of a partially recrystallized structure follows from the rule of mixtures

$$HV_c = X_V HV_{rex} + (1 - X_V) HV_{def} \qquad (1)$$

from the hardness of the deformed structure (HV_{def}) and that of the fully recrystallized structure (HV_{rex}). If the partial recrystallization (X_V=18%) of the as-received condition is taken into account, the recrystallized volume fraction corresponding to the hardness value of 390 HV10 during stagnation is estimated to 66%, in good agreement with the values determined by EBSD e.g. (65±2)% after annealing for 1872 h at 1150 °C (Fig. 2b).

In a similar manner, the time to half recrystallization can be estimated from the hardness evolution. The hardness value of half recrystallized material (X_V=0.5) is estimated to 406 HV10 from the hardness of the as-received and recrystallized condition taking into account the partial recrystallization in the as-received state. In the hardness evolution during isothermal annealing, this value occurs always between the two halting levels at 417±7 HV10 and 390±10 HV10. For each isothermal series, the time to half recrystallization is hence inferred by interpolation between the measured hardness values just before and after the sudden drop (for example, in case of 1150 °C, the hardness values at 168 h and 216 h). As illustrated in Fig 3, these estimated times to half recrystallization $t_{Xv=0.5}$ decrease with increasing temperature as expected for a thermal activated process. The consistency between the determined times to half recrystallization for different temperatures confirm that effects caused by the heterogeneity of the plate have been successfully confined to some extent.

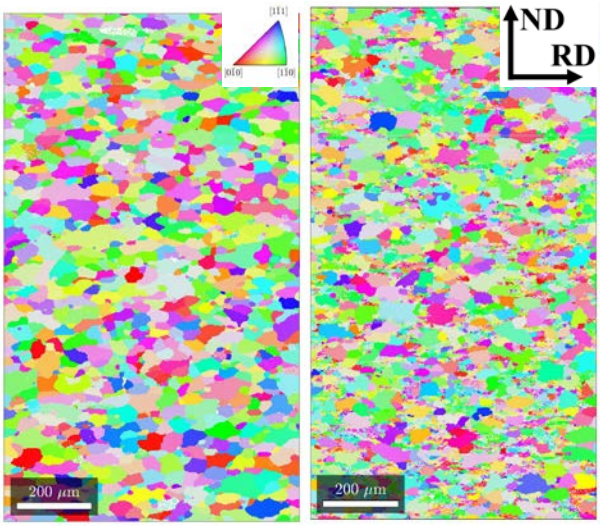

Fig. 2: Orientation maps obtained by EBSD on RD/ND sections of tungsten warm-rolled to 80% thickness reduction (W80) annealed for (a) 192 h at 1250 °C (fully recrystallized) and (b) 1872 h at 1150 °C (partially recrystallized with a recrystallized volume fraction of (65±2)%). The colors indicate the crystallographic direction along RD according to the insert. The rolling direction is horizontal; the top parts are closest to the center of the warm-rolled plate.

4. Discussion

Assessment of the thermal stability of the tungsten plate warm-rolled to 80% thickness reduction is partially hindered by the macroscopic heterogeneity and the partial recrystallization of the as-received condition. An attempt has been made to limit the influence of the heterogeneity, but as seen from the non-monotonous behaviour in the hardness evolution, this was not always successful. Analysis of the recrystallization kinetics is hence limited to an analysis of the time to half recrystallization $t_{Xv=0.5}$. As seen from Fig. 3, the dependence on temperature T follows accurately an Arrhenius relation

$$t_{X_V=0.5} = t^*_{X_V=0.5} \exp\left(\frac{Q}{RT}\right) \qquad (2)$$

with a prefactor $t^*_{Xv=0.5}$ and the ideal gas constant R. The activation energy Q of 548 kJ/mol obtained by fitting compares well with the one (579±7% kJ/mol) reported for the slightly less warm-rolled plate W67 [7] and the activation energy of bulk self-diffusion in polycrystalline tungsten (506-586 kJ/mol) [1], but it is significantly higher than the observed activation energy (352±4% kJ/mol) for the more severely warm-rolled plate

W90 [8] or that of short-circuit diffusion in tungsten (377-460 kJ/mol) [1]. The behaviour of W80 warm-rolled to 80% thickness reduction resembles more that of the plate warm-rolled to 67% thickness reduction than the one warm-rolled to 90% thickness reduction. The transition in activation energy for the time to half recrystallization from the one of bulk diffusion at low rolling reductions to the one of short-circuit diffusion at higher rolling reductions observed earlier occurs obviously not before 80% thickness reduction.

For all investigated temperatures, the time to half recrystallization reported here for W80 is shorter than the one of W67. This is mainly due to the larger driving force given by the larger stored energy density in the deformation structure as reflected also in the higher hardness of the as-received condition of W80, despite the apparent partial recrystallization. Due to the partial recrystallization of the as-received condition, the time to half recrystallization reported here must be considered only to be an estimate and would have to be corrected for the time span to reach the recrystallized volume fraction of X_V=18% of the as-received state. This time span would be governed also by thermal activated processes and depend on the annealing temperature; neglecting it, does not alter the apparent activation energy presuming the same governing processes through the late and early stages of recrystallization. Despite all mentioned problems with the heterogeneity of the plate, the occurrence of a period of time in which the hardness decrease halted and the process of recrystallization stagnated was clearly revealed. The time span, during which the processes halted, increases with decreasing temperature and lasted for the lowest temperature of 1150 °C for more than two months without leading to complete recrystallization as evidenced by Fig. 2b. The reason for such stagnation in the process of recrystallization is not obvious and one might speculate that particular texture components in the deformation structure might be harder to be invaded by moving grain boundaries carrying recrystallization (e.g. [16]). This might be either caused by a low mobility of the moving boundaries due to orientation pining or a low driving force for boundary motion due to significantly lower stored energy density (either as a result of plastic deformation during warm-rolling or caused by recovery during annealing).

5. Conclusions and outlook

During annealing of tungsten warm-rolled to 80% thickness reduction, the hardness does not decrease continuously and intervals of stagnation were identified. During these periods of time the hardness evolution and the progress of recrystallization halted. These halting periods turn even more relevant for assessing the suitability of the warm-rolled tungsten plates for future fusion applications. Neither complete recrystallization, nor full degradation of the mechanical properties occurs before recrystallization commences after the end of the halting period, deeming the W80 plate more suitable for application as armor material than expected solely from the time to half recrystallization and the inferred activation energy of 548 kJ/mol. It is envisaged, that the phenomenon of halted recrystallization discovered here could enable the design of deformed tungsten material which even not being unaffected by recrystallization, survive at the high operation temperatures in a partially recrystallized state not undergoing complete recrystallization for extended periods of time.

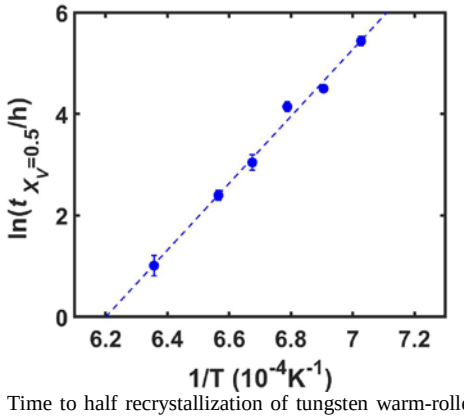

Fig. 3: Time to half recrystallization of tungsten warm-rolled to 80% thickness reduction as determined from the hardness evolution in dependence on annealing temperature (Arrhenius plot).

Acknowledgements

This work has been carried out partially within the framework of the EUROfusion Consortium and has received funding from the Euratom research and training program 2014-2018 under grant agreement No 633053. The views and opinions expressed herein do not necessarily reflect those of the European Commission.

Literature

[1] E. Lassner, W.-D. Schubert, The Element Tungsten, in: Tungsten, 1999: pp. 1–59.

[2] R.G. Abernethy, Mater. Sci. Technol. 0836 (2016) 1–12.

[3] J. Davis, V. Barabash, A. Makhankov, L. Plöchl, K. Slattery, J. Nucl. Mater. 258–263 (1998) 308–312.

[4] J. Reiser, J. Hoffmann, U. Jäntsch, M. Klimenkov, S. Bonk, C. Bonnekoh, M. Rieth, A. Hoffmann, T. Mrotzek, Int. J. Refract. Met. Hard Mater. 54 (2016) 351–369.

[5] B. Gludovatz, S. Wurster, A. Hoffmann, R. Pippan, Int. J. Refract. Met. Hard Mater. 28 (2010) 674–678.

[6] D. Rupp, S.M. Weygand, J. Nucl. Mater. 386–388 (2009) 591–593.

[7] A. Alfonso, D. Juul Jensen, G.N. Luo, W. Pantleon, J. Nucl. Mater. 455 (2014) 591–594.

[8] A. Alfonso, D. Juul Jensen, G.N. Luo, W. Pantleon, Fusion Eng. Des. 98–99 (2015) 1924–1928.

[9] K. Wang, X. Zan, M. Yu, W. Pantleon, L. Luo, X. Zhu, P. Li, Y. Wu, Fusion Eng. Des. 125 (2017) 521–525.

[10] M. Yu, K. Wang, X. Zan, W. Pantleon, L. Luo, X. Zhu, Y. Wu, Fusion Eng. Des. 125 (2017) 531-536.

[11] K. Tsuchida, T. Miyazawa, A. Hasegawa, S. Nogami, M. Fukuda, Nucl. Mater. Energy. 15 (2018) 158–163.

[12] U.M. Ciucani, A. Thum, C. Devos, W. Pantleon, Nucl. Mater. Energy. 15 (2018) 128-134.

[13] T. Palacios, J. Reiser, J. Hoffmann, M. Rieth, A. Hoffmann, J.Y. Pastor, Int. J. Refract. Met. Hard Mater. 48 (2015) 145–149.

[14] S. Bonk, J. Reiser, J. Hoffmann, A. Hoffmann, Int. J. Refract. Met. Hard Mater. 60 (2016) 92–98.
[15] J. Reiser, M. Rieth, B. Dafferner, A. Hoffmann, J. Nucl. Mater. 423 (2012) 1–8.
[16] Z. Zhang, Y. Zhang, O. V. Mishin, N. Tao, W. Pantleon, D. Juul Jensen, Metall. Mater. Trans. A. 47 (2016) 4682–4693.